Eur Biophys J (2007) 36:1039–1048
DOI 10.1007/s00249-007-0173-z

ORIGINAL PAPER

Kinetics of the electron transfer reaction of Cytochrome c_{552} adsorbed on biomimetic electrode studied by time-resolved surface-enhanced resonance Raman spectroscopy and electrochemistry

Sophie Bernad · Nadine Leygue · Hafsa Korri-Youssoufi · Sophie Lecomte

Received: 14 February 2007 / Revised: 23 April 2007 / Accepted: 24 April 2007 / Published online: 5 June 2007

Abstract Cytochrome c_{552} (Cyt-c_{552}) and its redox partner ba_3-oxidase from *Thermus thermophilus* possess structural differences compared with *Horse heart* cytochrome *c* (cyt-*c*)/cytochrome *c* oxidase (CcO) system, where the recognition between partners and the electron transfer (ET) process is initiated via electrostatic interactions. We demonstrated in a previous study by surface-enhanced resonance Raman (SERR) spectroscopy that roughened silver electrodes coated with uncharged mixed self-assembled monolayers $HS–(CH_2)_n–CH_3/HS–(CH_2)_{n+1}–OH$ 50/50, $n = 5$, 10 or 15, was a good model to mimic the Cyt-c_{552} redox partner. All the adsorbed molecules are well oriented on such biomimetic electrodes and transfer one electron during the redox process. The present work focuses on the kinetic part of the heterogeneous ET process of Cyt-c_{552} adsorbed onto electrodes coated with such mixed SAMs of different alkyl chain length. For that purpose, two complementary methods were combined. Firstly cyclic voltammetry shows that the ET between the adsorbed Cyt-c_{552} and the biomimetic electrode is direct and reversible. Furthermore, it allows the estimation of both the density surface coverage of adsorbed Cyt-c_{552} and the kinetic constants values. Secondly, time-resolved SERR (TR-SERR) spectroscopy showed that the ET process occurs without conformational change of the Cyt-c_{552} heme group and allows the determination of kinetic constants. Results show that the kinetic constant values obtained by TR-SERR spectroscopy could be compared to those obtained from cyclic voltammetry. They are estimated at 200, 150 and 40 s^{-1} for the ET of Cyt-c_{552} adsorbed onto electrodes coated with mixed SAMs $HS–(CH_2)_n–CH_3/HS–(CH_2)_{n+1}–OH$ 50/50, $n = 5$, 10 or 15, respectively.

Keywords Cytochrome c_{552} · Surface-enhanced resonance Raman spectroscopy · Time-resolved SERS · Self-assembled monolayers · Coated electrodes

Introduction

Cytochromes *c* act as electron carriers between cytochrome *c* reductase (complexes III) and cytochrome *c* oxidase (complexes IV, *CcO*) in the respiratory chain of prokaryotic and eukaryotic organisms. For the eukaryotic cytochrome *c* from *horse heart* (cyt-*c*), it is well established that the surface recognition and the electron transfer process with its redox partners occur through electrostatic interactions between the positive lysine-rich domain around the exposed heme edge and the specific negatively charged binding domains around the binuclear Cu_A center of the redox partners (Scott and Mauk 1995).

Such a cationic domain was regarded as a common structural template for soluble *c*-type cytochromes until it was shown that cytochrome c_{552} (Cyt-c_{552}) from *Thermus thermophilus* (Soulimane et al. 1997) does not exhibit a cluster of lysine residues on the protein surface close to the heme edge (Than et al. 1997). Cyt-c_{552} possesses also a more stable structure compared with cyt-*c*, brought about

Presented at the joint biannual meeting of the SFB-GEIMM-GRIP, Anglet France, 14–19 October, 2006.

S. Bernad · N. Leygue · S. Lecomte (✉)
LADIR, CNRS/UPMC (UMR 7075), 2 rue Henri Dunant, 94320 Thiais, France
e-mail: sophie.lecomte@glvt-cnrs.fr

H. Korri-Youssoufi
Equipe de Chimie Bioorganique et Bioinorganique, Institut de Chimie Moléculaire et des Matériaux d'Orsay, UMR-CNRS 8182, Bâtiment 420, université Paris-Sud XI, 91405 Orsay, France

by ca. 1/3 of the C-terminal peptide chain that wraps around the remainder of the protein (Than et al. 1997). This largely uncharged peptide segment (Met63-Leu75) partly shields the heme pocket on the front surface of the protein. In contrast to other cytochromes c oxidases, the putative binding domain of ba_3-oxidase from *Thermus thermophilus*, around the Cu_A center, lacks any negatively charged residues as revealed by the crystal structure (Soulimane et al. 2000; Than and Soulimane 2001). Those unique structural properties of ba_3-oxidase and Cyt-c_{552}, therefore, raises fundamental questions with respect to the recognition and the molecular mechanism of the electron transfer between both partners. Moreover, there is no cross-reactivity with *horse heart* cyt-*c* (Soulimane et al. 1997). Specifically, it has to be determined if a conformational rearrangement of the heme for the biological electron transfer may be also of relevance for the reaction of Cyt-c_{552} with the ba_3-oxidase, as suggested for the cyt *c*/*CcO* redox couple (Döpner et al. 1999; Hildebrandt and Stockburger 1989a, b). Recently, we characterized the redox properties of Cyt-c_{552} adsorbed on different self-assembled thiol monolayers (SAMs) grafted on silver electrode, used to model the chemical environment of the redox partner (Bernad et al. 2004, 2006). The use of silver electrode allows us to employ surface-enhanced resonance Raman (SERR) spectroscopy, which selectively probes the vibrational spectrum of the heme group solely of the adsorbed Cyt-c_{552} (Lecomte et al. 1999, 1998a). It appears in our study that the surface, which mimics in a better way the environment of the ba_3-oxidase, is a mixed SAMs formed by polar (Ag–$(CH_2)_n$–CH_2OH) and hydrophobic (Ag–$(CH_2)_n$–CH_3) alkanethiols. Only the native form, B1(6cLS) of Cyt-c_{552}, is detected by SERRS when the protein is adsorbed on such a surface. This surface promotes a protein orientation favorable for the electron transfer. We demonstrated that the number of transferred electron was close to 1, concluding that all the adsorbed heme proteins were electroactive and had the same orientation. Most likely the uncharged residues close to the edge interact with the mimetic surface. The electron transfer between the modified electrode and Cyt-c_{552} is not dependent on a structural change of the heme (Bernad et al. 2006).

In the present study, we have used a combination of two complementary techniques: electrochemistry and time-resolved surface-enhanced resonance Raman (TR-SERR) spectroscopy, to examine the kinetics of the heterogeneous electron transfer between Cyt-c_{552} and the silver electrode coated with mixed (hydrophilic/hydrophobic) SAM of various alkyl chain lengths, used as a biomimetic surface of its redox partner (ba_3-oxidase). Surface-enhanced Raman (SER) spectroscopy is a powerful technique to study the conformation of the heme group of Cyt-c_{552} adsorbed on the electrode. Because of the selective enhancement of the Raman scattering upon adsorption on electrochemically roughened metal electrodes (Ag, Au, Cu), it can be used to probe exclusively the molecular structure of the species in the electrical double layer (Cotton et al. 1980). This technique has been successfully used to study the potential-dependent equilibrium of the heme proteins, where the SER effect and molecular resonance Raman (RR) effect can be combined (SERR) (Hildebrandt and Stockburger 1989a, b). Under these conditions, the sensitivity is further increased and the measured spectra exclusively display the vibrational bands of the heme group (i.e., the redox center) from the adsorbed heme protein. Stationary potential-dependent SERR measurements provide information on the thermodynamics (E°) of the interfacial redox process as well as the redox active site structures of the adsorbed species involved.

SERR spectroscopy has been extended to the time-resolved domain by combining the SERR spectroscopic measurements with the potential jump technique (Lecomte et al. 1998b; Wackerbarth et al. 1999). Thus, it is possible to probe the kinetics of the electron transfer of heme proteins in the millisecond time scale (Lecomte et al. 1999). Cyclic voltammetry experiments have been performed on a coated silver electrode, with the same roughness as that of the electrode previously used for SERR experiments, in order to determine the redox potential of adsorbed Cyt-c_{552}, the reversibility of the electrochemical process, the amount of adsorbed Cyt-c_{552} and the rate constant of the electron transfer. The correlation of the redox and kinetics properties obtained by both techniques was demonstrated. The mixed surfaces (Ag–$(CH_2)_n$–CH_2OH) /(Ag–$(CH_2)_n$–CH_3) lead to a homogeneous orientation of Cyt-c_{552} and a fast electron transfer reaction between the heme and the coated electrode. These experiments reveal that the interaction of Cyt-c_{552}/ba_3-oxidase is governed by a different driving force compared to the redox couple cyt-*c*/cytochrome *c* oxidize.

Experimental

Chemicals: 1-Hexanethiol (HS–$(CH_2)_5$–CH_3), 1-undecanethiol (HS–$(CH_2)_{10}$–CH_3), 1-hexadecanethiol (HS–$(CH_2)_{15}$–CH_3), 6-mercapto-1-hexanol (HS–$(CH_2)_6$–OH) and 11-mercapto-1-undecanol (HS–$(CH_2)_{11}$–OH) were purchased from Aldrich and were used without further purification; 16-mercapto-1-hexadecanol was synthesized in our laboratory. Purification of Cyt-c_{552} from *Thermus thermophilus* was carried out according to published procedures (Than et al. 1997).

Preparation of the silver electrode

The silver electrode used was constituted of planar plate or cylinder ring depending on the measurement and was

prepared as follows: after mechanical polishing, the silver electrode was transferred into the electrochemical cell containing 0.1 M KCl. Three double potential steps from –0.3 to +0.3 V (90, 30, 30 s) were applied for the oxidation and the reduction of the silver electrode, which was then rinsed with water. The real surface of the roughened silver electrode was evaluated using a limiting diffusion method, based on the electrochemical measurement of the limiting current at a constant anodic potential of the FeII/FeIII redox couple, in a solution of $K_4Fe(CN)_6$ (1 mM) and $K_3Fe(CN)_6$ (1 mM) in 0.1 M KCl. Therefore, the effective surface area could be evaluated from the Cottrell equation $I_d(t) = nFAD^{1/2}Co/(\pi^{1/2}t^{1/2})$ (where I_d means the diffusion current, D the diffusion coefficient, n the number of exchanged electrons, F the Faraday's constant, Co the concentration of the redox species and A the real area of the electrode).

From the value of the diffusion current, we were able to estimate the effective surface area for the plate electrode to be 17 cm^2. The simple geometrical area measured being 2 cm^2, the surface roughness factor for this silver electrode was subsequently estimated to be 8.5.

Preparation of coated electrodes

The roughened silver electrodes were immersed in 1 mM ethanolic solutions of thiols $HS–(CH_2)_n–CH_3$/$HS–(CH_2)_{n+1}–OH$ (50/50 v/v) for three alkyl chain lengths (n = 5, 10, 15) for 18 h. The silver rings were then rinsed with ethanol and dried under a stream of nitrogen. The modified electrode was placed for 30 or 90 min in a solution containing 0.2 μM Cyt-c_{552} in a buffer 10 mM Tris/HCl with 50 mM KCl (pH = 7.6).

Electrochemistry

Cyclic voltammetry experiments were performed in a glass cell incorporating a conventional three-electrode configuration using a silver plate (prepared as described above) as the working electrode, a platinum mesh as the counter electrode and a saturated calomel electrode as reference. The supporting electrolyte solution was thoroughly deoxygenated using oxygen-free argon prior to the electrochemical measurements. An autolab PGSTAT 100 potentiostat controlled by GPES autolab software was used for electrochemical measurements.

The total charges Q_i exchanged between adsorbed Cyt-c_{552} and the coated electrodes were determined from coulometric integration of the anodic peaks on the voltammograms. Hence, the following relationship has been used to obtain the surface densities Γ_i of Cyt-c_{552} adsorbed onto the coated electrodes:

$$Q_i = n\ F\ \Gamma_i\ S$$

with n: number of transferred electron, F: the Faraday constant and S: the surface of the electrode estimated to 17 cm^2.

The kinetic constants of the electron transfer process were calculated from the voltammograms using the analytical method of Laviron applied to adsorbed systems (Laviron 1979).

Stationary SERR spectroscopy and TR-SERR spectroscopy

The silver working electrode is a homemade rotating one, constructed according to a previously published description (Hildebrandt et al. 1988). Due to the rotation of the working electrode, the laser beam does not locally heat the sample. Platinum and saturated calomel electrodes were used as counter and reference electrodes, respectively. All potentials cited in this work refer to the saturated calomel electrode (SCE). The laboratory-built three-electrode cell was connected to an EG&G 273A potentiostat. SERR spectra were recorded at ambient temperatures with the 413.1 nm excitation line of a Spectra Physics Kr ion laser. The spectrograph (Dilor XY) is equipped with a liquid nitrogen cooled CCD camera and is used with a high dispersive system (spectral resolution of 2 cm^{-1} and step width of 0.8 cm^{-1}). The laser beam (ca. 40 mW) was focused onto the surface of the rotating Ag electrode. The total accumulation time of the SERR spectra varied between 30 and 180 s.

In time-resolved experiments, a rapid potential jump (<<100 μs) from an initial potential E_i to a final potential E_f was imposed and the SERR spectra were measured after (variable) delay times δ with a time interval Δt of 5 ms. After this measuring interval, the potential was set back to E_i in order to establish the initial equilibrium. The sequence was repeated N times (from 500 to 2000) until the effective total accumulation $N \times \Delta t$ time was between 2, 5 and 10 s as required for a sufficient signal-to-noise ratio. The time resolution was controlled by gated excitation rather than gate signal detection. A Pockel cell, synchronized with the potential jump trigger, achieved gating of the laser beam.

Results and discussion

Reversible electron transfer

Cyclic voltammograms (CV) obtained for Cyt-c_{552} adsorbed on a roughened silver electrode modified with $HS–(CH_2)_{n+1}–OH$/ $HS–(CH_2)_n–CH_3$, 50/50, with n = 5,

10 and 15, were recorded in 0.01 M Tris–HCl buffer (pH 7.6) with 0.05 M KCl as function of the scan rate from 0.02 to 10 V s^{-1}. Figure 1 presents the CV for Cyt-c_{552} adsorbed on SAMs with an alkyl chain length of 10. The electrochemical response of Cyt-c_{552} shows a well-defined one-electron redox wave. The peak separation varies up to 220 mV in the studied scan range from 0.02 to 10 V s^{-1}, and the full width at half height (fwwh) is around 110 mV. These results show that the redox process can be regarded as reversible, as the theoretical reversible process for adsorbed electroactive species correspond to a zero-peak separation and an fwwh of 90.6 mV (Bard and Faulkner 2001).

Figure 2 shows the variation of the anodic and cathodic currents as a function of the scan rate. Both cathodic and anodic peak currents vary linearly with the scan rate, which demonstrates that the Cyt-c_{552} is anchored at the surface of the modified electrode. The same behavior for Cyt-c_{552}, adsorption on the modified electrode and reversibility of the electron transfer, is observed for the other alkyl chain lengths of the SAMs, $n = 5$ or $n = 15$.

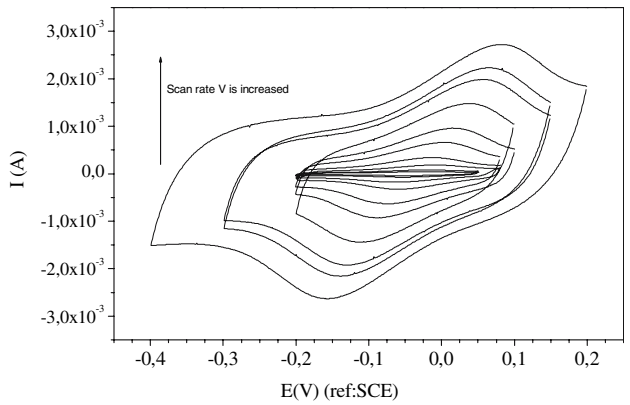

Fig. 1 Cyclic voltammogramm of Cyt-c_{552} adsorbed on coated (HS–$(CH_2)_{10}$–CH_3/HS–$(CH_2)_{11}$–OH, 50/50) roughened silver electrode obtained in de-oxygenated 0.01 M Tris/HCl buffer (pH 7.6) with 0.05 M KCl at potential scan rates of 0.1, 0.2, 0.5, 1, 2, 3, 5, 7, 8, 10 V s^{-1}. For the different voltammograms, the scan rate is increased in the direction of the *arrow*

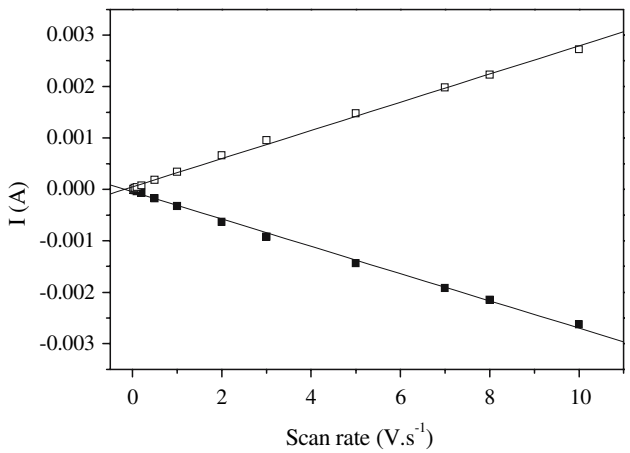

Fig. 2 Variations of the anodic and cathodic peak currents of Cyt-c_{552} adsorbed on coated (HS–$(CH_2)_{10}$–CH_3/HS–$(CH_2)_{11}$–OH, 50/50) roughened silver electrode as a function of the potential scan rate

The formal potential for the Cyt-c_{552} immobilized on the silver electrode modified with HS–$(CH_2)_{11}$–OH/ HS-$(CH_2)_{10}$–CH_3, calculated as the average of the observed anodic and cathodic peak potentials, is –0.033 V vs. SCE (0.207 V vs. NHE) and is independent of the scan rate in the whole range. Table 1 lists the formal potential for the Cyt-c_{552} adsorbed on the different chain lengths of SAM obtained by cyclic voltammetry ($E°(V)^a$). The values are all close to the potential of Cyt-c_{552} in solution (–0.038 V vs. SCE) (Hon-Nami and Oshim 1977) leading to assume that the structure of the heme protein and the heme edge are not modified by the adsorption process.

The coulometric integration of the anodic peak allows to estimate the amount of electroactive Cyt-c_{552} adsorbed on mixed SAM (HS–$(CH_2)_{n+1}$–OH/HS–$(CH_2)_n$–CH_3, $n = 5$, 10 and 15), as described in the experimental section. Considering a one electron transfer process and a surface area of 17 cm^2 (after correction of the roughness factor), the density of surface coverage of the biomimetic electrodes by Cyt-c_{552} is 2, 10 and 6 pmol.cm^{-2} for mixed SAM (50/50) of HS–$(CH_2)_{5+1}$–OH/ HS–$(CH_2)_5$–CH_3, HS–$(CH_2)_{10+1}$–OH/ HS–$(CH_2)_{10}$–CH_3 and HS–$(CH_2)_{15+1}$–OH/ HS–$(CH_2)_{15}$–CH_3 respectively. Assuming that the protein keeps a structure close to its native crystalline structure and that the available surface of one molecule is 1400 $Å^2$ (Than et al. 1997), the theoretical value for a coverage density of the electrode with a monolayer of protein would be 12 pmol cm^{-2}. We can deduce from our results that around a monolayer of Cyt-c_{552} is adsorbed onto the modified electrode by HS–$(CH_2)_{10+1}$–OH/ HS–$(CH_2)_{10}$–CH_3. For the other chain lengths, less than a monolayer of Cyt-c_{552} is adsorbed.

These values can be compared to those obtained for cytochrome *c* from *horse heart* (cyt-*c*) when adsorbed on ω-carboxylalkanethiols SAMs grafted on smooth gold electrodes. This surface, known as the electrostatic model, is indeed described as a good model for the recognition site of cytochrome *c* oxidase for cyt-*c*. On such surfaces, a surface density corresponding to one monolayer is estimated from electrochemical techniques whatever the chain length of the SAM is (Clark and Bowden 1997; Feng et al. 1995, 1997; Song et al. 1993). In the case of rat heart, cytochrome *c* adsorbed on mixed SAMs of alkanethiols and ω-terminated alkanethiols (terminated with pyridine, imidazole or nitrile), very low coverage density is observed, corresponding to a 10% of the theoretical value of the monolayer (Wei et al. 2002). Those terminated groups

Table 1 Characteristic parameters ($E°$, k_1, density of surface) of Cyt-c_{552} adsorbed on mixed SAM-coated Ag electrodes (HS–$(CH_2)_n$–CH_3/HS–$(CH_2)_{n+1}$-OH 50/50 v/v, n = 5, 10, 15) obtained by cyclic voltammetry[a] and SERRS[b]. A driving force E_f–E_0 = –0.03 V was applied for the determination of rate constants by SERRS measurements

SAM	$E°$ (V)[a] (vs. SCE)	$E°$ (V)[b] (vs. SCE)	Density of surface[a] (10^{-12} mol cm^{-2})	k_1^a (s^{-1})	k_1^b (s^{-1})
n = 5	– 0.055 ± 0.010	+ 0.009 ± 0.006	2 ± 1	208 ± 20	>200
n = 10	– 0.033 ± 0.014	–0.010 ± 0.004	11 ± 2	165 ± 42	150 ± 50
n = 15	– 0.073 ± 0.010	–0.042 ± 0.005	6 ± 2	39 ± 19	10 ± 5

are indeed able to ligate to the heme and to make the surface coverage lower than a monolayer when used in mixed SAMs.

Using cyclic voltammetry we were able to detect a direct electron transfer process between adsorbed Cyt-c_{552} and electrode coated with SAM, HS–$(CH_2)_{n+1}$–OH/ HS–$(CH_2)_n$–CH3, n = 5, 10 or 15, whatever the chain length of the SAM is. We also established that this electron transfer is reversible for the three SAMs used.

Conformation of Cyt-c_{552} adsorbed on mixed SAM

T. thermophilus Cyt-c_{552} may present several configurations of the porphyrin group, depending on the experimental conditions, as previously described (Bernad et al. 2004; Lecomte et al. 1998a). In the native form called B1, the heme structure shows a six-coordinated low-spin (6cLS) configuration, with Met-69 and His-15 as axial ligands. Resonance Raman spectra in the range 1300–1600 cm^{-1} are specific of the porphyrin groups (Hu et al. 1993) and give information on the oxidation, spin and coordination of the heme iron (marker bands ν_4, ν_3, ν_2, ν_{11} and ν_{37}).

When Cyt-c_{552} is adsorbed onto the surface of a roughened silver rotating electrode, the protein can exist in a conformational equilibrium between the two states, B1 and B2 (Lecomte et al. 1998a). The B1 state exhibits essentially the same spectrum as the native dissolved Cyt-c_{552}, and the nonnative state B2 comprises a five-coordinated high-spin B2(5cHS) and a six-coordinated low-spin B2(6cLS) form. B2 species are only observed when Cyt-c_{552} is adsorbed on the naked silver surface, but with a very small contribution. The spectral parameters of the pure spectra B1 and B2 species have already been determined and the main marker bands are listed in Table 2. The SERR spectra of Cyt-c_{552} adsorbed on a mixed self-assembled monolayer (HS–$(CH_2)_{n+1}$–OH/ HS–$(CH_2)_n$–CH_3, 50/50) in equilibrium condition at different potentials are shown in Figs. 3 and 4, for n = 5 and n = 15, respectively. A quantitative analysis of SERRS spectra leads to the determination of the percentage of each conformation of Cyt-c_{552} heme adsorbed on mixed SAM as described in previous papers (Bernad et al. 2004, 2006). The native B1 states (oxidized and reduced) are the more favored conformations. No B2ox(5cHS) state is detected on the electrode. The B2(6cLS) is observed at the oxidized state (at potential +0.05 or +0.01 V). However, the percentage is less than 10%, whatever the chain length of the SAM is.

Using the Nersnt equation, the redox potential of Cyt-c_{552} adsorbed on SAM were determined from a quantitative analysis of the SERR spectra recorded at different potentials in stationary conditions (Bernad et al. 2004). The values are listed in Table 1 ($E°$(V)[b]). It appears that for the same chain length, the values of the formal potential calculated from the voltammograms are more negative from 20 to 60 mV than those obtained by SERRS spectroscopy. These variations could be due to different experimental conditions used in both methods. In the case of SERR spectroscopy, the shape of the working electrode is not the same as that for cyclic voltammetry, whereas the counter and the reference electrodes are identical. In addition, there is incertitude in the determination of the maximum of the peak potential in the voltammograms, due to the large shape of the peaks. Finally, we neglect the B2 conformations for the determination of the redox potential by SERR spectroscopy, whereas those species are present in the spectra (less than 10%). Besides, a study by Clark and Bowden showed that the potential values for horse heart cytochrome *c* adsorbed on carboxylic acid terminated SAMs grafted on gold electrodes are more negative when the protein is more strongly adsorbed (Clark and Bowden 1997). In our study, the adsorption time differs slightly for the SERR experiments (30 min) and for the cyclic voltammetry experiments (90 min), which could have led to a more strongly adsorbed form in the latter case and would explain the more negative values obtained by cyclic voltammetry measurements. An adsorption time of 30 min. was indeed not sufficient to get an exploitable signal in cyclic voltammetry.

The redox potential becomes more negative when the chain length of the SAM is increased. According to Battistuzzi et al. it could be due to a more hydrated heme crevice, as the chain length is increased (Battistuzzi et al. 2002). The longer the chain length, the smoother is the surface onto which the Cyt-c_{552} is adsorbed and the less specific is the interaction between the protein and the SAM, as also observed by Leopold and Bowden (2002).

Table 2 Wavenumbers (cm^{-1})and relatives intensities (in parentheses) of the main marker bands of the dissolved (B1 state) and the adsorbed (B2 state) forms of Cyt-c_{552}

Mode	$B1_{red}$	$B1_{ox}$	$B2_{red}$6cLS	$B2_{ox}$6cLS	$B2_{red}$5cHS	$B2_{ox}$5cHS
ν_4	1360.8 (1.000)	1370.5 (1.000)	1360.1 (1.000)	1376.7 (1.000)	1353.6 (1.000)	1371.4 (1.000)
ν_3	1491.6 (0.073)	1501.0 (0.223)	1492.8 (0.045)	1506.8 (0.206)	1468.5 (0.164)	1490.0 (0.613)
ν_{11}	1540.0 (0.108)	1557.5 (0.141)	1545.9 (0.094)	1568.8 (0.581)	1565.1 (0.037)	1553.8 (0.293)
ν_2	1588.0 (0.265)	1581.0 (0.362)	1589.8 (0.145)	1586.2 (0.847)	ND	1574.5 (0.374)

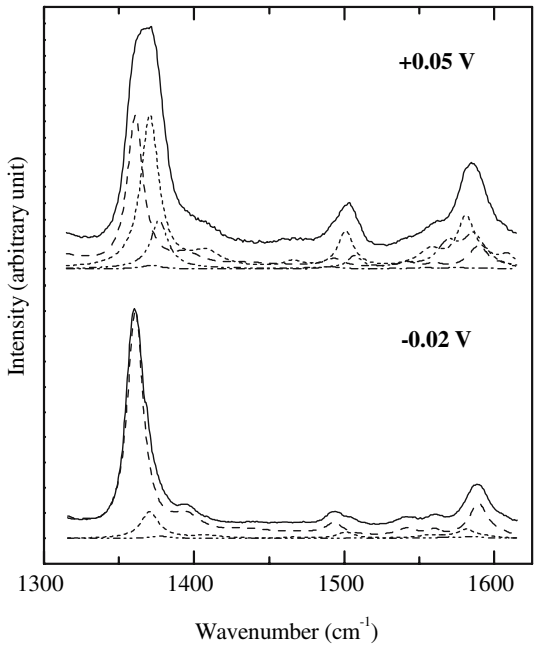

Fig. 3 Stationary SERR spectra of Cyt-c_{552} adsorbed on Ag electrodes coated with HS–$(CH_2)_5$–CH_3/HS–$(CH_2)_6$–OH (1:1, v/v), excited at 413 nm and recorded at two different potentials (*solid line*). The *dashed*, *dotted* and *dashed-dotted* lines refer to the fitted component of the reduced and oxidized B1(6cLS) forms and of the B2(6cLS) oxidized form, respectively

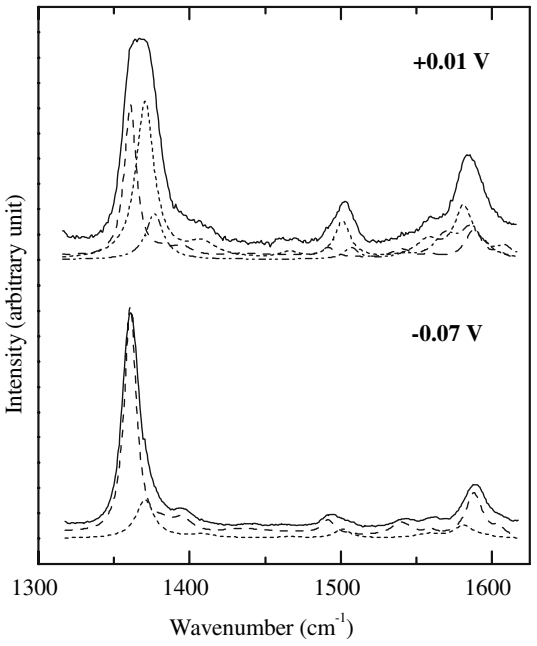

Fig. 4 Stationary SERR spectra of Cyt-c_{552} adsorbed on Ag electrodes coated with HS–$(CH_2)_{15}$–CH_3/HS–$(CH_2)_{16}$–OH (1:1, v/v), excited at 413 nm and recorded at two different potentials (*solid line*). The *dashed*, *dotted* and *dashed-dotted* lines refer to the fitted component of the reduced and oxidized B1(6cLS) forms and of the B2(6cLS) oxidized form, respectively

SERR spectroscopy furnishes information complementary to electrochemistry by giving the structure of the heme group of Cyt-c_{552} adsorbed onto the biomimetic electrodes. Combining both methods allows us to conclude that the heme of Cyt-c_{552} adsorbed onto electrodes coated with SAM, HS–$(CH_2)_{n+1}$–OH/HS–$(CH_2)_n$–CH_3, n = 5, 10 or 15, keeps its native structure (6cLS) when it transfers electron to the biomimetic electrode in a reversible manner.

Kinetics of electron transfer

For the time-resolved SERR measurements, Cyt-c_{552} was adsorbed on SAM covered electrode at –0.4 V to ensure that the protein was exclusively in the state B1, as checked by a stationary SERR experiment. Subsequently, the potential was set to the initial potential *E*i to start the time-resolved experiments. The initial dwell time at *E*i (Ca. 5 s) was sufficiently long to establish the redox equilibrium of B1. After each time-resolved experiment, a stationary SERR spectrum was measured at –0.4 V. Except for a slight lowering of the total intensity, these spectra reveal no differences compared to those measured prior to the time-resolved experiments. Thus, any denaturizing process of the adsorbed Cyt-c_{552} could be ruled out.

The range of the potential jumps was chosen to obtain large differences between the equilibrium concentration of reduced Cyt-c_{552} in the native form (B1red) and oxidized Cyt-c_{552} in the native form (B1ox) at the initial and final potentials E_i and E_f, which are essential for a reliable quantitative analysis of the time-resolved SERR spectra. Because of the oxidation potential of Ag/AgCl and the concomitant loss of SERR activity at potentials close to $E°$ (Ag/AgCl), a value close to 0.0 V constitutes the upper limit for the accessible potentials. For the short SAMs, the

E_i value was set to +0.05 V and for long SAM at +0.01 V. The $E°$ (B1red/B1ox) of Cyt-c_{552} adsorbed on mixed SAM were determined from stationary SERRS measurements at +0.009 and –0.042 V (ref SCE) for $n = 5$ and $n = 15$, respectively. Consequently, E_f were chosen to have negative values (–0.02 and –0.07 V) to increase the percentage of B1red, leading to an increase in the driving force for the heterogeneous reduction.

Figures 5 and 6 show a selection of time-resolved SERR spectra measured at various delay times for Cyt-c_{552} adsorbed on short ($n = 5$) and long ($n = 15$) mixed SAM. As expected, the reduced B1 increases at the expense of B1ox with increasing delay times. On the other hand, the contribution of the non-native oxidized form B2(6cL) is small and varies little with the delay time. These results are in agreement with previous results obtained on a naked electrode, where it was shown that the conformational transition B1ox to B2ox was much slower than the electron transfer of B1 (Lecomte et al. 1998b). The data analysis can be restricted to the electron transfer process based on a one-step relaxation mechanism, i. e. $e^- + \text{B1ox} \underset{k_2}{\overset{k_1}{\rightleftarrows}} \text{B1red}$. One expresses the rate of the reaction as

$$\mathrm{d}(C_{\mathrm{B1red}})/\mathrm{d}t = k_1 C_{\mathrm{B1ox}} - k_2 C_{\mathrm{B1red}} \tag{1}$$

and the equilibrium constant of the reaction to be

$$K_{\mathrm{eq}}(E_f) = \frac{k_1}{k_2} = \exp\left(-(E_f - E^\circ)\frac{nF}{RT}\right) \tag{2}$$

Combination of both relationships (1) and (2) gives:

$$\ln \frac{(C_{\mathrm{B1red}}(t) - C_{\mathrm{B1red}}(E_f))}{(C_{\mathrm{B1red}}(E_i) - C_{\mathrm{B1red}}(E_f))} = -(k_1 + k_2)t = f(t) \tag{3}$$

with $k_1 + k_2 = p$ and finally

$$k_1 = \frac{p * K_{\mathrm{eq}}}{1 + K_{\mathrm{eq}}} \tag{4}$$

and

$$k_2 = \frac{p}{1 + K_{\mathrm{eq}}} \tag{5}$$

The obtained kinetic constants k_1 are given in Table 1. The values of 150 s^{-1} and 10 s^{-1} were found for Cyt-c_{552} adsorbed onto the electrode coated with HS–$(CH_2)_{n+1}$–OH/HS–$(CH_2)_n$-CH_3, $n = 10$ and 15, respectively. For the electron transfer between Cyt-c_{552} and the electrode coated with the shortest SAMs HS–$(CH_2)_{5+1}$–OH/HS–$(CH_2)_5$–CH_3, only an estimation of the rate constant could be calculated. By comparing the kinetic spectrum at $\delta = 0$ ms (Fig. 5) and the stationary spectrum at +0.05 V (Fig. 3), we can observe that all the oxidized B1 species had been converted to the reduced B1 species. It means that the electron transfer process is almost complete when the first spectrum can be taken with this setup ($\delta = 0$ ms). The electron transfer process is too fast to be studied with this experimental setup when Cyt-c_{552} is adsorbed onto the electrode coated with the shortest SAMs. The electron transfer rate between Cyt-c_{552} and the modified silver electrode were also calculated from the cyclic voltammograms using the method of Laviron (Laviron 1979). The obtained values are listed in Table 1 and vary from 208 s^{-1} for the shortest chain length to 39 s^{-1} for the longest one. These results show that both techniques (electrochemistry and SERRS) give the electron transfer rate in the same order of magnitude.

Kinetic parameters for the heterogeneous electron transfer of Cyt-c_{552} adsorbed onto electrodes coated with HS–$(CH_2)_{n+1}$–OH/HS–$(CH_2)_n$–CH_3 are compared to those obtained in the case of cyt-c adsorbed onto electrodes modified with ω-carboxylalkanethiols HS–$(CH_2)_n$–COOH. Murgida and Hildebrandt calculated by TR-SERR spectroscopy that the kinetic constants for the electron transfer process between horse heart cytochrome c and Ag electrodes coated with HS–$(CH_2)_n$–COOH, $n = 5$, 10, 15 were 134, 43 and 0.073 s^{-1} respectively (Hildebrandt and Murgida 2002; Murgida and Hildebrandt 2001). Kinetic constant values around 100 and 0.1 s^{-1} measured with Laviron's method from cyclic voltammetry are found when cyt-c is adsorbed on Au–S–$(CH_2)_n$–COOH, for $n = 10$ and $n = 15$ (El Kasmi et al. 1998; Feng et al. 1997; Song et al. 1993). As for electron transfer rates with Au–S–$(CH_2)_5$–COOH, Wei et al. measured a kinetic constant of 680 s^{-1} for rat heart cytochrome c using Marcus model with cyclic voltammetry (Wei et al. 2004). By electroreflectance spectroscopy, a kinetic constant value of 1100 s^{-1} has been determined for cyt-c adsorbed on Au–S–$(CH_2)_5$–COOH (Feng et al. 1997). For long distance electron transfer processes (chain length with $n \geq 10$) experience has shown that the kinetic rate depends exponentially on the distance according to Marcus' theory (Avila et al. 2000; Marcus and Sutin 1985; Murgida and Hildebrandt 2004). The mechanism is hence controlled by electron tunnelling. At short distances (chain length with $n < 9$), the electron transfer process becomes distance independent and a conformational rearrangement is the rate limiting step (Avila et al. 2000; Jeuken 2003). When cyt-c was coordinatively bound to pyridine-terminated alkanethiols SAMS on Au or Ag electrodes, Yue et al. (2006) demonstrated that at short distances the electron transfer mechanism seemed to be controlled by solvent/protein friction instead of a gated process. It is understood from those studies that several parameters intervene in the electron transfer process, which is a complex phenomenon not fully understood yet.

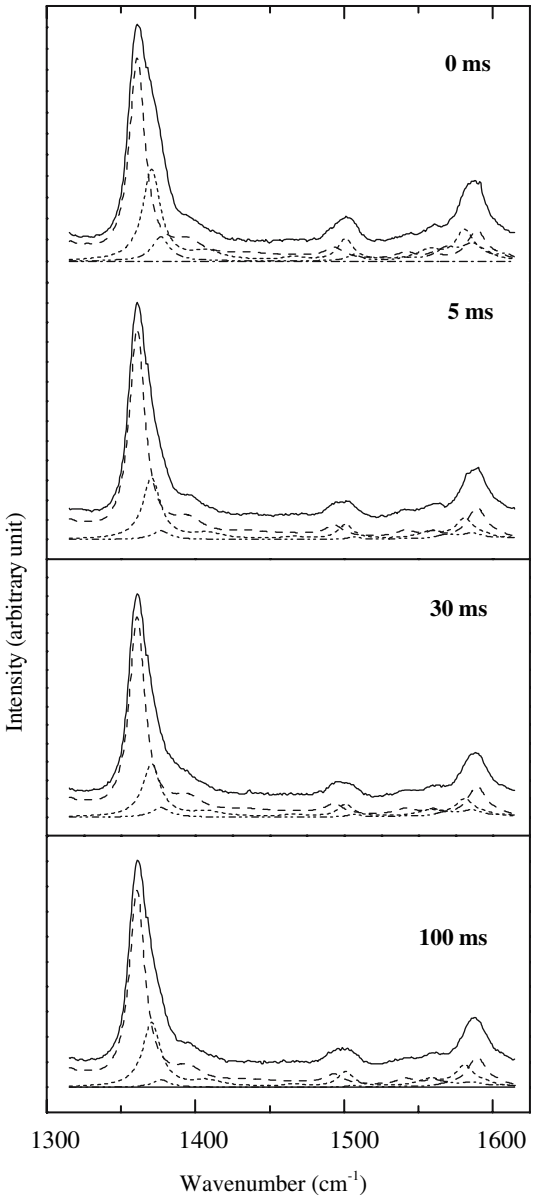

Fig. 5 Time-resolved SERR spectra of the Cyt-c_{552} adsorbed on Ag electrodes coated with HS–$(CH_2)_5$–CH_3/HS–$(CH_2)_6$–OH (1:1, v/v) for a potential jump from 0.05 to 0.02 V measured at various delay times δ'. The excitation wavelength was 413 nm, the number of cycle was 1,000 and 2,000. The *dashed*, *dotted* and *dashed-dotted* lines indicate the component spectra of the reduced and oxidized B1(6cLS) forms and of the B2(6cLS) oxidized form, respectively

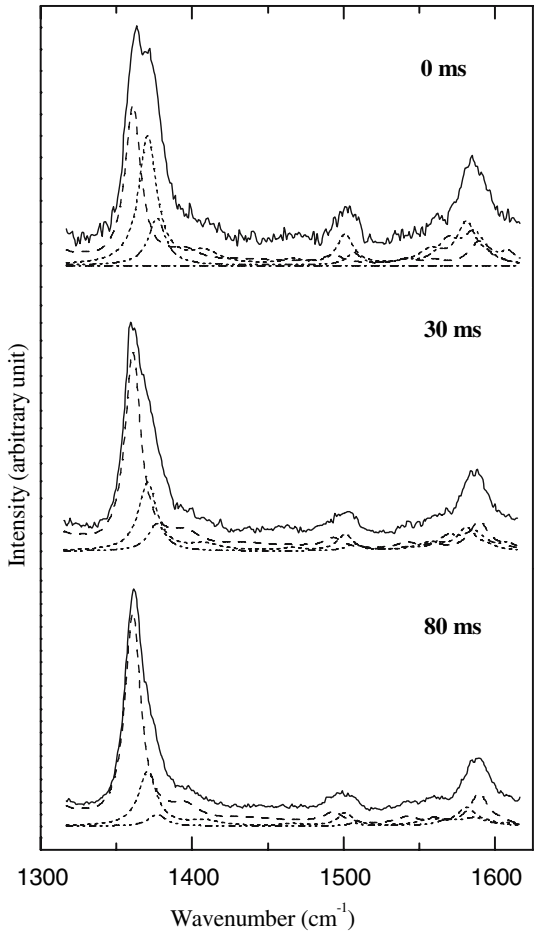

Fig. 6 Time-resolved SERR spectra of the Cyt-c_{552} adsorbed on Ag electrodes coated with HS–$(CH_2)_{15}$–CH_3/HS–$(CH_2)_{16}$–OH (1:1, v/v) for a potential jump from 0.01 to –0.07 V measured at various delay times δ'. The excitation wavelength was 413 nm, the number of cycle was between 1,000 and 2,000. The *dashed*, *dotted* and *dashed-dotted* lines indicate the component spectra of the reduced and oxidized B1(6cLS) forms and of the B2(6cLS) oxidized form, respectively

Kinetic constant values are greater for cyt-*c* than for Cyt-c_{552} when the proteins are adsorbed onto electrodes coated with SAMs of shortest alkyl chain length, Au–S–$(CH_2)_5$–COOH and Ag–S–$(CH_2)_{n+1}$–OH/Ag–S–$(CH_2)_n$–CH_3 for cyt-*c* and Cyt-c_{552}, respectively. The chosen method for the measurements, cyclic voltammetry for Cyt-c_{552} and electroreflectance study for cyt-*c*, could be responsible for this difference in kinetic constant values. It appears also from our work that the kinetic constants obtained for Cyt-c_{552} adsorbed onto electrodes coated with longer mixed SAMs HS–$(CH_2)_{n+1}$–OH/ HS–$(CH_2)_n$–CH_3 (n = 10 and n = 15) are larger than those observed for cyt-*c* adsorbed on the electrostatic model, with the same chain lengths, i.e., electrode coated with HS–$(CH_2)_n$–COOH. The heterogeneous electron transfer between Cyt-c_{552} and the electrode coated with mixed SAMs is hence faster than the electron transfer between cyt-*c* and the electrostatic model. It seems that the mixed SAMs mimic in a better way the redox partner of Cyt-c_{552} than the electrostatic model does for cyt-*c*.

Conclusion

We have studied the kinetics of the electron transfer of Cyt-c_{552} adsorbed on biomimetic electrodes by combining two different methods: time-resolved SERR spectroscopy and

cyclic voltammetry. These two methods are complementary. Cyclic voltammetry has shown that the electron transfer process between adsorbed Cyt-c_{552} and the electrode coated with mixed SAMs, HS–$(CH_2)_{n+1}$–OH/HS–$(CH_2)_n$–CH_3 50/50 was reversible and direct between both partners, but no structural information of heme group of Cyt-c_{552} could be obtained. For that purpose, time-resolved SERR spectroscopy was used to determine the conformations of the electroactive species of Cyt-c_{552} adsorbed onto the modified electrode. Furthermore, estimations of the thermodynamic (redox potential) and the kinetic (rate constant for the electron transfer) parameters of the heterogeneous electron transfer were calculated by both methods and demonstrate that the obtained results are in the same range.

Our studies confirm that the electrode coated with mixed SAMs HS–$(CH_2)_{n+1}$-OH/HS–$(CH_2)_n$–CH_3 50/50 is a good model to mimic the properties of the Cyt-c_{552} redox partner, ba_3-oxidase from *Thermus thermophilus*. Cyt-c_{552} molecules adsorbed onto these biomimetic electrodes are well oriented and exhibit quickly all their native conformation. In addition, the electron transfer process is fast and reversible. By varying the chain length of the SAMs, we have also established that adsorbing Cyt-c_{552} onto a short chain length should improve the rate of the electron transfer.

By combining two complementary methods, we have characterized the electron transfer process between Cyt-c_{552} and the electrode coated with mixed SAMs. These mixed SAMs are hence shown to be good starting points for elaborating a more complex biomimetic model of the Cyt-c_{552} redox partner and could be used to study further what parameters control the electron transfer mechanism.

Acknowledgment The authors thank Dr Tewfik Soulimane for the gift of Cyt-c_{552}.

References

Avila A, Gregory BW, Niki K, Cotton TM (2000) An electrochemical approach to investigate gated electron transfer using a physiological model system: cytochrome *c* immobilized on carboxylic acid-terminated alkanethiol self-assembled monolayers on gold electrodes. J Phys Chem B 104:2759–2766

Bard AJ, Faulkner LR (2001) Electrochemical methods: fundamentals and applications. Wiley, New York

Battistuzzi G, Borsari M, Cowan JA, Ranieri A, Sola M (2002) Control of cytochrome *c* redox potential: axial ligation and protein environment effect. J Am Chem Soc 124:5315–5324

Bernad S, Soulimane T, Lecomte S (2004) Redox and conformational equilibria of cytochrome *c*552 from *Thermus thermipohilus* adsorbed on chemically modified silver electrode probed by SERR spectroscopy. J Raman Spectrosc 35:47–54

Bernad S, Soulimane T, Lecomte S (2006) Characterization and redox properties of cytochrome *c*552 from *Thermus thermophilus* adsorbed on different self-assembled thiol monolayers, used to model the chemical environment of the redox partner. Biopolymers 81:407–418

Clark RA, Bowden EF (1997) Voltametric peak broadening for cytochrome *c*/alkanethiolate monolayer structures: dispersion of formal potentials. Langmuir 13:559–565

Cotton TM, Schultz SG, Van Duyne RP (1980) Surface-enhanced resonance Raman scattering from cytochrome *c* and myoglobin adsorbed on a silver electrode. J Am Chem Soc 102:7960–7962

Döpner S, Hildebrandt P, Rosell FI, Mauk AG, von Walter M, Buse G, Soulimane T (1999) The structural and functional role of lysine residues in the binding domain of cytochrome *c* in the electron transfer to cytochrome c oxidase. Eur J Biochem 261:379–391

El Kasmi A, Wallace JM, Bowden EF, Binet SM, Linderman RJ (1998) Controlling interfacial electron transfer kinetics of cytochrome *c* with mixed self-assembled monolayers. J Am Chem Soc 120:225–226

Feng ZQ, Imabayashi S, T. K, Niki K (1995) Electroreflectance spectroscopic study of the electron transfer rate of cytochrome c electrostatically immobilized on the o-carboxyl alkanethiol monolayer modified gold electrode. J Electroanal Chem 394:149–154

Feng ZQ, Imabayashi S, Kakiushi T, Niki K (1997) Long-range electron-transfer reaction rates to cytochrome across long- and short- chain alkanethiol self-assembled monolayers: electroreflectance studies. J Chem Soc Faraday Trans 93:1367–1370

Hildebrandt P, Macor KA, Czernuszewicz RS (1988) Novel cylindrical rotating electrode for anaerobic surface-enhanced Raman spectroscopy. J Raman Spectrosc 19:65–69

Hildebrandt P, Murgida DH (2002) Electron transfer dynamics of cytochrome *c* bound to self-assembled monolayers on silver electrodes. Bioelectrochemistry 55:139–143

Hildebrandt P, Stockburger M (1989a) Cytochrome *c* at charged interfaces 1: conformational and redox equilibria at the electrode/electrolyte interface probed by surface-enhanced resonance Raman spectroscopy. Biochemistry 28:6710–6721

Hildebrandt P, Stockburger M (1989b) Cytochrome *c* at charged interfaces 2: complexes with negatively charged macromolecular systems studied by resonance Raman spectroscopy. Biochemistry 28:6722–6728

Hon-Nami K, Oshim T (1977) Purification and some properties of cytochrome *c*552 from an extreme thermophile, *Thermus thermophilus*. J Biochem 82:769–776

Hu S, Morris IK, Singh JP, Smith KM, Spiro TG (1993) Complete assignment of cytochrome *c* resonance Raman spectra via enzymatic reconstitution with isotopically labeled hemes. J Am Chem Soc 115:12446–12458

Jeuken LJC (2003) Conformational reorganisation in interfacial protein electron transfer. Biochim Biophys Acta 1604:67–76

Laviron E (1979) General expression of the linear potential sweep voltammogram in the case of diffusionless electrochemical systems. J Electroanal Chem 101:19–28

Lecomte S, Hildebrandt P, Soulimane T (1999) Dynamics of the heterogeneous electron-transfer reaction of cytochrome c_{552} from *Thermus thermophilus*. A time-resolved surface-enhanced resonance Raman spectroscopic study. J Phys Chem B 103:10053–10064

Lecomte S, Wackerbarth H, Hildebrandt P, Soulimane T, Buse G (1998a) Potential-dependent surface-enhanced resonance Raman spectroscopy of cytochrome c_{552} from *Thermus thermophilus*. J Raman Spectrosc 29:687–692

Lecomte S, Wackerbarth H, Soulimane T, Buse G, Hildebrandt P (1998b) Time-resolved surface-enhanced resonance Raman spectroscopy for stuying electron -transfer dynamics of heme proteins. J Am Chem Soc 120:7381–7382

Leopold MC, Bowden EF (2002) Influence of gold substrate topography on the voltammetry of cytochrome c adsorbed on carboxylic acid terminated self-assembled monolayers. Langmuir 18:2239–2245

Marcus RA, Sutin N (1985) Electron transfers in chemistry and biology. Biochim Biophys Acta 811:265–322

Murgida DH, Hildebrandt P (2001) Proton-coupled electron transfer of cytochrome *c*. J Am Chem Soc 123:4062–4068

Murgida DH, Hildebrandt P (2004) Electron-transfer processes of cytochrome *c* at interfaces: new insights by surface-enhanced resonance Raman spectroscopy. Acc Chem Res 37:854–861

Scott RA, Mauk AG (1995) Cytochrome c: a multidisciplinary approach. University Science Books, Sausalito

Song S, Clark RA, Bowden EF (1993) Characterization of cytochrome *c*/alkanethiolate structures prepared by self-assembly on gold. J Phys Chem 97:6564–6572

Soulimane T, Buse G, Bourenkov GP, Bartunik HD, Huber R, Than ME (2000) Structure and mechanism of the aberrant ba_3-cytochrome c oxydases from *Thermus thermophilus*. EMBO Journal 19:1766–1776

Soulimane T, Von Walter M, Hof P, Than ME, Huber R, Buse G (1997) Cytochrome c_{552} from *Thermus thermophilus*: a functional and crystallographic investigation. Biochemical and Biophysical Research Commun 237:572–576

Than ME, Hof P, Huber R, Bourenkov GP, Bartunik HD, Buse G, Soulimane T (1997) *Thermus thermophilus* cytochrome c_{552}: a new highly thermostable cytochrome *c* structure obtained by MAD phasing. J Mol Biol 271:629–644

Than ME, Soulimane T (2001) Ba_3-Cytochrome *c* oxydase from *Thermus thermophilus*. In: Messerschmidt A, Huber R, Poulos T, Wieghardt K (eds) Handbook of metalloproteins, Chichester, pp 363–378

Wackerbarth H, Klar U, Günther W, Hildebrandt P (1999) Novel time-resolved surface-enhanced (resonance) Raman spectroscopic technique for studying the dynamics of interfacial processes: application to the electron transfer reaction of cytochrome *c* at silver electrode. Appl Spectrosc 53:283–291

Wei J, Liu AR, Yamamoto H, He Y, Waldeck DH (2002) Direct wiring of cytochrme *c*'s heme unit to an electrode: electrochemical studies. J Am Chem Soc 124:9591–9599

Wei JJ, Liu H, Niki K, Margoliash E, Waldeck DH (2004) Probing electron tunneling pathways: electrochemical study of rat heart cytochrome *c* and its mutant on pyridine-terminated SAMs. J Phys Chem B 108:16912–16917

Yue H, Khoshtariya D, Waldeck DH, Grochol J, Hildebrandt P, Murgida DH (2006) On the electron transfer mechanism between cytochrome c and metal electrodes: evidence for dynamics control at short distances. J Phys Chem B 110:19906–19913